

# PCCP

Accepted Manuscript



This is an *Accepted Manuscript*, which has been through the Royal Society of Chemistry peer review process and has been accepted for publication.

*Accepted Manuscripts* are published online shortly after acceptance, before technical editing, formatting and proof reading. Using this free service, authors can make their results available to the community, in citable form, before we publish the edited article. We will replace this *Accepted Manuscript* with the edited and formatted *Advance Article* as soon as it is available.

You can find more information about *Accepted Manuscripts* in the [Information for Authors](#).

Please note that technical editing may introduce minor changes to the text and/or graphics, which may alter content. The journal's standard [Terms & Conditions](#) and the [Ethical guidelines](#) still apply. In no event shall the Royal Society of Chemistry be held responsible for any errors or omissions in this *Accepted Manuscript* or any consequences arising from the use of any information it contains.

## ARTICLE

# Fluorinated graphene dielectric films obtained from functionalized graphene suspension: preparation and properties

Cite this: DOI: 10.1039/x0xx00000x

Received 14th October 2014,  
Accepted 00th

DOI: 10.1039/x0xx00000x

[www.rsc.org/](http://www.rsc.org/)N. A. Nebogatikova<sup>a</sup>, I. V. Antonova<sup>a,b</sup>, and V. Ya. Prinz<sup>a</sup>, I. I. Kurkina<sup>c</sup>, V. I. Vdovin<sup>a</sup>, G. N. Aleksandrov<sup>c</sup>, V. B. Timofeev<sup>c</sup>, S. A. Smagulova<sup>c</sup>, E. R. Zakirov<sup>a</sup>, V. G. Kesler<sup>a</sup>

In the present study, we have examined the interaction between a suspension of graphene in dimethylformamide and an aqueous solution of hydrofluoric acid, which was found to result in partial fluorination of suspension flakes. A considerable decrease in the thickness and lateral sizes of the graphene flakes (up to 1-5 monolayer in thickness and 100-300 nm in diameter) with increasing the duration of fluorination treatment is found to be accompanied with simultaneous transition of the flakes from conducting to insulating state. Smooth and uniform insulating films with roughness  $\sim 2$  nm and thicknesses down to 20 nm were deposited from the suspension on silicon. The electrical and structural properties of the films suggest their use as insulating elements in thin-film nano- and microelectronics device structures. In particular, it was found that the films prepared from the fluorinated suspension display rather high breakdown voltages (field strength of  $(1-3) \times 10^6$  V/cm), ultra low densities of charges in the film and at the interface with silicon substrate in metal-insulator-semiconductor structures ( $\sim (1-5) \times 10^{10}$  cm<sup>-2</sup>). Such excellent characteristics of the dielectric film can be compared only to well developed SiO<sub>2</sub> layers. The films from the fluorinated suspension are cheap, practically feasible and easy to produce.

## Introduction

Graphene and graphene-based materials have attracted huge practical and theoretical interest of many researchers [1]. The possibility to create lateral and vertical quantum structures, and also the possibility to controllably tune the properties of such structures, is just one reason for studying graphene and obtaining, by means of chemical modification, graphene-based materials with new promising properties [1-3]. The bandgap opening in the energy spectrum of graphene is a most important and called-for modification of this material. Another important problem in graphene functionalization is the search for means that would allow control of material parameters of graphene and its derivatives.

The most widely known chemical derivatives of graphene are fluorinated graphene, hydrogenated graphene, and oxidized graphene. All those materials are high-resistivity or dielectric materials with bandgap energy in excess of 3 eV. As it was shown in a number of studies, the above materials show different stability of their properties [4-8]. The most stable material (in terms of thermal and time stability) is fluorinated graphene [5], hydrogenated and oxidized graphenes being less stable derivatives [4,9]. On the other hand, the possibility of the initial properties restoration for materials makes chemically

modified graphene derivatives attractive for use in device structures.

For chemical modification of graphene aimed at obtaining fluorinated graphene, treatments of the material in gaseous atmosphere or in plasma are most frequently used. In all cases, favorable conditions for the reaction of graphene with fluorine involve high temperatures and pressures, and also using toxic substances, both circumstances making the fluorination process a difficult technological task [4-8]. The mentioned technological problems restrict the use of fluorinated graphene. Generally, large-scaled preparation of fluorographene or fluorinated graphene with a possibility to control the fluorination degree remains a great challenge. An easy-operating, highly scalable and low-cost approaches were reported on for the preparation of fluorographene [for instant, 10]. Earlier, we developed a simple and easy process for graphene fluorination at room temperature and atmospheric pressure in an aqueous solution of hydrofluoric acid (HF) [11,12] which proved to be a process offering a possibility to manage the fluorination degree of graphene and few-layer graphene sheets.

Nowadays, the methods for graphene obtaining include electrostatic or mechanical cleaving of graphite [13,14], growth of graphene layers by chemical vapor deposition [2,15], and chemical exfoliation of graphite (preparation of suspensions)

[16,17]. The approach using the preparation of graphene suspensions is the cheapest method for obtaining graphene and producing large-area graphene films; yet, such films usually show only a limited quality. One of the main problems here is to achieve splitting of graphite in monolayers without using of chemical oxidation, and with demand of reducing of such suspensions or suspension-based films [16, 17]. Very often, obtained graphene suspensions contain particles in the form of graphite flakes several ten nanometers thick. Fluorination of suspensions was implemented for graphene oxide at elevated temperatures and pressures as well; as a result, oxifluorographene suspensions were obtained [3,7,18].

The purpose of the present work was to apply our new approach for graphene fluorination (the treatment in aqueous solution of HF [11,12,19]) for graphene suspensions, and to study the interaction of graphene suspensions with aqueous solutions of hydrofluoric acid. This study aimed at structural and chemical modification of suspension flakes, at obtaining fluorinated graphene suspensions with various fluorination degrees, and at creation and characterization of the films from these suspensions. In the course of fluorination procedure, we have discovered an unexpected phenomenon that consisted in additional splitting of suspension flakes in much thinner and finer elements in comparison with initial flakes. This phenomenon has allowed us to create uniform and thin large-area dielectric films. It was found that thin films (thickness 100 - 20 nm, roughness ~ 2 nm) obtained from a fluorinated graphene suspension offer many useful dielectric material properties; namely, and, first of all, they exhibit high breakdown voltages and very low densities of charges in the film and at the interface with silicon in metal-insulator-semiconductor structures ( $\sim 5 \times 10^{10} \text{ cm}^{-2}$ ). Both properties make such films promising candidates for use as insulating elements in thin-film device structures.

### The experimental methods for graphene suspension creation, modification and characterization

The starting material was a graphene suspension that was obtained by a standard procedure described in [5,16,17]. The main stages in the preparation of the suspension were the following: mechanical crushing of natural graphite, dimethylformamide (DMF) intercalation, ultrasonic treatment intended for splitting the intercalated particles, and centrifugation intended for removal of non-split graphite particles. In preparation of the suspension, the natural graphite was turned into particles with characteristic sizes 1 to 2  $\mu\text{m}$  (length and width) and up to 20 - 70 nm (thickness).

After the graphene suspension was obtained, it was subjected to a fluorination procedure. To this end, equal volumes of the graphene suspension and a 5 % solution of hydrofluoric acid (HF) in water were mixed together. Periodically, some portions of the suspension were used for the study and preparation of films. The substrates for films were silicon (Si) wafers. In depositing the films, the native oxide was removed from the surface of silicon by the hydrofluoric acid available in the

solution. The deposited films were dried and rinsed with deionized water for removing the residual hydrofluoric acid and the organic component of the suspension, and then they were given a second drying treatment for water removal.

The properties of the films formed on silicon substrates were studied using the following experimental techniques: scanning electron microscopy (SEM), Raman scattering spectroscopy (RSS), X-ray photoelectron spectroscopy (XPS), atomic force microscopy (AFM), and measurement of capacitance-voltage and current-voltage characteristics. For taking AFM images of the film and substrate surfaces and for determining the film thicknesses, a Solver PRO NT-MDT scanning microscope was used. Measurements were performed both in contact and semi-contact mode. Raman spectra were measured at room temperature, the excitation wavelength being 514.5 nm (2.41-eV argon ion laser). In order to avoid the heating of samples with laser-emitted radiation, the laser beam power was decreased to 2-3 mW. The spectra were recorded using an NT MDT Nanolaboratory INTEGRA Spectra spectrometer. SEM images were taken using a JEOLJSM-7800F scanning electron microscope with the energy of primary electrons equal to 2 keV. Structural features of the sample(s) were examined by transmission electron microscopy (TEM, JEM-2200FS, 200kV accelerating voltage). For measuring XPS spectra, an SSC Riber facility (Surface Science Centre Riber) was used. Measured XPS spectra permitted studying the chemical composition of obtained films. Fourier transform infrared (FTIR) absorbance spectra were recorded using a Varian 7000 FTIR spectrometer. Sixteen scans of each spectrum were taken using a range of 4000–550  $\text{cm}^{-1}$  at a resolution of 8  $\text{cm}^{-1}$ . For measuring capacitance-voltage and current-voltage characteristics, an E7-20 immitancemeter and a Keithley picoammeter (model 6485) were used. The electrical contacts to the films were prepared by sputtering Au onto the film surface, the contact surface area being 0.5  $\text{mm}^2$ . In this way, a set of vertical metal-insulator-semiconductor (MIS) Au/fluorinated graphene/Si structures was obtained.

### The structure of fluorinated graphene films with various fluorination degrees

Films were prepared by means of pour droplets of suspension on the silicon substrate with drying, rinsing in deionized water for removing the residual hydrofluoric acid and the organic component of the suspension, and a second drying treatment for water removal. We have to notice that addition of an aqueous solution of HF to a suspension changed the wettability of the silicon substrates with respect to suspension droplets: the fluorinated suspension easily spread over the surface of substrate to form a thin continuous film.

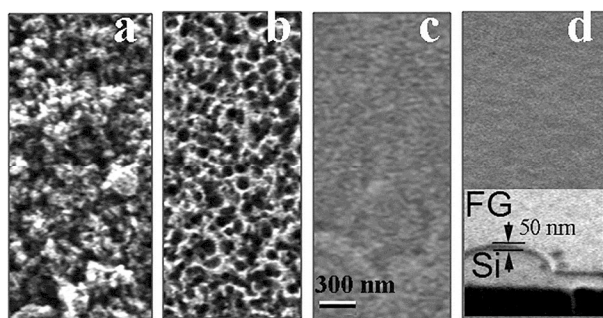


Fig. 1. SEM images of the surface of films fluorinated in the aqueous solution of HF during different times. The scales in the images are identical. a – pristine (non-fluorinated) film; b, c, and d – films fluorinated respectively during 2, 10, and 40 days. The inset in Fig. 1 d shows an image of an edge of the film taken at the angle 45° to the surface; the film thickness indicated in the figure was evaluated with allowance for measurement geometry.

By means of scanning electron and atomic force microscopy, we showed that the characteristic particle sizes in the formed films and the thicknesses of the films themselves depended on the time during which the suspension was treated in the aqueous solution of HF. Figure 1 a-d presents scanning microscopy data that prove that treatments of suspensions in an aqueous solution of HF led to improved uniformity of the surface of obtained films and to a relief reduction on the film surface. The thickness of the films formed on the surface of silicon from droplets containing identical amounts of suspension decreased with increasing the treatment duration: after 25-day fluorination treatment, films 150 to 100 nm thick (respectively at the center and at the periphery of the sample) where obtained, whereas after 40-day fluorination treatment the film thickness decreased to 80-50 nm (see the inset to Fig. 1 d). The minimal thickness of obtained continuous films was 20 nm. The typical thickness of films treated during 60-70 days was ~50-40 nm.

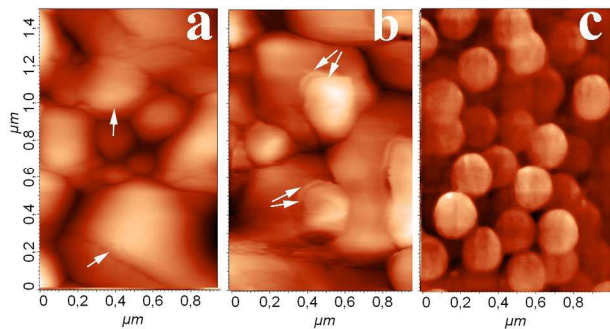


Fig. 2. AFM images of film surfaces. The films were obtained using suspensions of various fluorination degrees: a, b and c – a 4-day, 10-day and 70-day fluorination treatment, respectively. The splitting layers are shown with arrays.

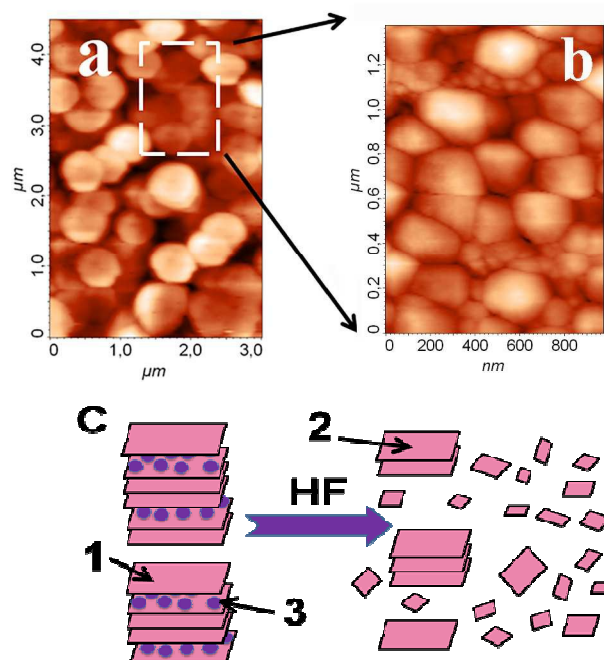


Fig. 3. AFM images of the surface for a film having been treated in the aqueous solution of HF during 60 days. In the image of Fig. 3 a, taken at a lower magnification, only large-scale particles are seen. In the image shown in Fig. 3 b, large and fine fluorographene nanosheets are seen. (c) A sketch illustrating the additional splitting of initial flakes and their fractionation in finer flakes that occurred during treatment of a suspension in an aqueous solution of hydrofluoric acid (1 – initial particle, 2 – split-off partially fluorinated flakes, 3 – intercalated DMF layer).

AFM images of the film surface after fluorination are shown in Fig. 2. Note the additional splitting of graphene flakes in the suspension that occurred during the treatment (see Fig. 2 a, b). One split off layer can be seen on each flake in Fig. 2a for 4-day treatment, and two split off layers can be seen on each flake in Fig. 2b for 10-day treatment. A comparison between the lateral and vertical sizes of the particles in Figs. 2 a and 2 c shows that those sizes decreased with increasing the duration of the treatment in the aqueous solution of HF. For better visualization of the processes proceeding during the treatment of the suspension, Figure 3 a, b shows images of films at different scales. It is seen that, in the suspension, particles of two characteristic sizes, 200 to 400 nm and 20 to 50 nm were present. The latter observation points to fractionation of initial into finer particles (for more detail, see Discussion). The obtained data on the lateral sizes and thicknesses of the large-scale flakes are shown in Fig. 4. The minimal sizes of these flakes after 80 - 120 days of fluorination were found to equal 100 to 300 nm (diameter) and 0.5 to 2.0 nm (thickness). Thus, the processes leading to the splitting and fragmentation of large into finer particles get decelerated or ceased over rather long times of the treatment. The finest flakes had characteristic sizes 20 to 50 nm, with their thickness exhibiting no noticeable dependence on treatment duration and their concentration increasing with increasing the duration of fluorination treatment.

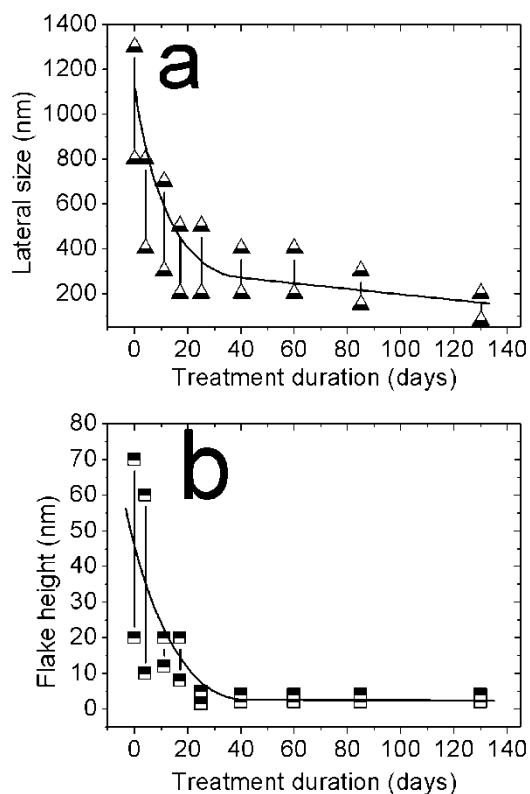


Fig. 4. The lateral sizes (a) and thickness (b) of suspension particles versus the duration of HF treatment. The solid line is added to the plots to facilitate data comprehension.

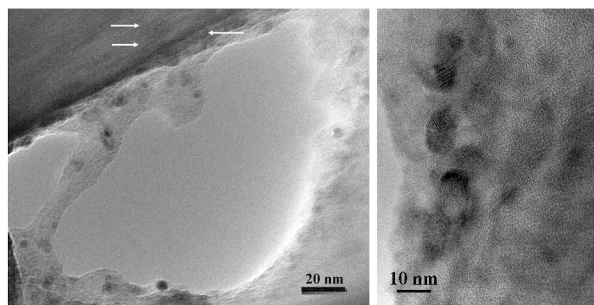


Fig. 5. TEM images of films treated in the aqueous solution of HF for 70 days in the multi-beam diffraction (left) and high resolution electron microscopy (right) modes. Arrows are marked some of the relatively large flakes.

Figure 5 demonstrates the TEM images one of the films. Rounded flakes are clearly seen in these images with relatively large (20-30 nm) and small sizes (5-10 nm). These images are in good agreements with the AFM data and suggested model (Figure 2 and 3).

### Evidences for the fluorination reaction of graphene flakes

One of the main evidence of fluorination is the transition from conductive to insulation properties of the films created from suspension treated in the aqueous solution of HF during more

than 25 days. In details the film insulated properties will be given in the next section.

During treatment of a graphene suspension in an aqueous solution of HF, changes of color visible with naked eye occurred in the suspension. The inset in Fig. 6 a shows a photo of two vessels, one (left) vessel containing a graphene suspension prior to fluorination treatment, and the other (right) vessel, a graphene suspension after the treatment. The change in suspension color was not due to sedimentation of a precipitate in the vessel since the color could not be restored by stirring the suspension. The change of suspension color observed on fluorination could be, in addition to reduced sizes of suspension particles, also due to the formation of fluorographene. Indeed, it is known that fluorinated graphene is a white substance with a bandgap width of 3.2 eV [5,18].

The gradual emergence of fluorinated graphene properties could be traced in measured Raman spectra of our samples. Prior to analyzing the effect of fluorination on the spectra, we would like to describe the Raman features observed in the spectra of pristine (non-fluorinated) samples. Known Raman features for graphene (graphite) are a weak D peak ( $1350\text{ cm}^{-1}$ ), G peak ( $1590\text{ cm}^{-1}$ ), and 2D peak ( $2690\text{ cm}^{-1}$ ). The Raman spectra of our samples contained a considerable contribution of D peak due to flake edges, so that the amplitude of the G peak was comparable with that of the D peak, the latter peak being forbidden in ideal graphene and graphite lattices. The emergence of a D peak in the Raman spectra of graphene films is due to  $sp^3$ -hybridized carbon atoms present in the films (carbon atoms with dangling bonds or atoms with chemical bonds outside the graphene sheet). Also, the Raman spectra additionally contained peaks due to DMF and its derivatives. In the Raman spectra of our samples, those features were  $1445$  and  $2930\text{ cm}^{-1}$  peaks due to differently deformed DMF molecules. The  $1445\text{ cm}^{-1}$  peak is known to be due to the asymmetric bending of carbon-hydrogen bonds in the  $\text{CH}_2$  "molecule", and the  $2930\text{ cm}^{-1}$  peak, due to the stretching vibrations of such bonds [20,21]. Moreover, the  $1445$  and  $2930\text{ cm}^{-1}$  peaks were observed for molecules containing  $\text{CH}_2$  fragments. Note that, for the C-N bond, a peak around  $1430\text{ cm}^{-1}$  can also be expected [22]. It is worth noting that no such peaks were observed in graphene and few-layer graphene films obtained by electrostatic exfoliation of graphite and in graphene and few-layer graphene films grown by chemical vapor deposition (CVD) [11,12].

Raman spectra measured on the films obtained from suspensions fluorinated during different times are shown in Fig. 6 b. It is seen that an increased duration of the treatment of the suspension in the aqueous solution of HF resulted in a decreased intensity of peaks in Raman spectra, this effect is typical for fluorination of graphene [5,18]. The latter modification of Raman spectra was due to the opening of a bandgap in fluorographene ( $\sim 3.0 - 3.5\text{ eV}$ ), resulting in that the excitation energy ( $2.41\text{ eV}$ ) was no longer sufficient for the occurrence of band-to-band electron transitions. The gradual decrease of the amplitude of Raman peaks implies that the

fluorination degree of the films gradually increased with treatment duration.

A concomitant weakening of DMF-induced peaks at 1445 and 2930  $\text{cm}^{-1}$  also deserves mention. Most probably, this observation means that the solution of HF penetrated inside the few-layer graphene films along DMF intercalation planes. The presence of water in the solution promoted the decomposition of DMF into constituents and the release of heat during the decomposition. Owing to the heat released during DMF decomposition the fluorination reaction was promoted. Fluorination of the graphene led to a local modification of carbon atoms hybridization, to a change of lattice constant, to an emergence of mechanical stress, and to a change in the reactivity of the immediate surrounding. Graphene fluorination led also to a local change in the graphene layers wettability. Those changes acted to promote the penetration of the HF-containing solution into the graphene films, the spreading of fluorination reaction inside the flakes, and the additional splitting of flakes.

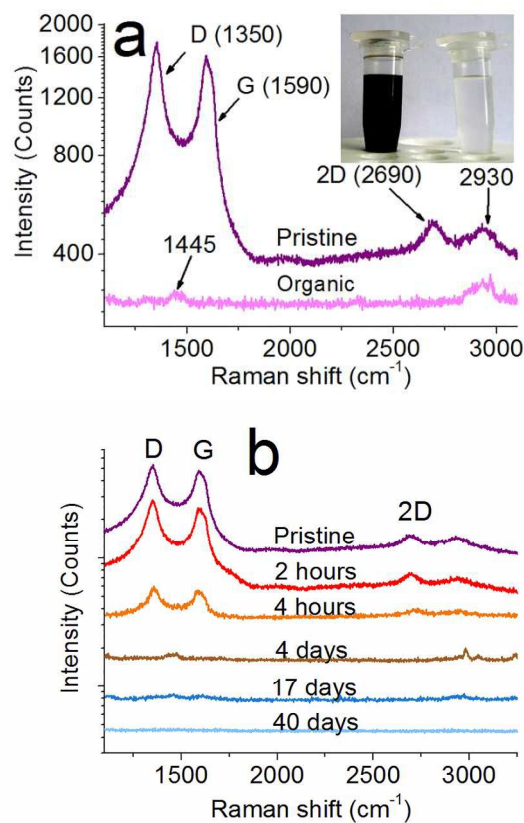


Fig. 6. (a) Typical Raman spectra of a pristine suspension and the organic solution component in the suspension. (b) Evolution of Raman spectra of pristine fluorinated films with the duration of HF treatment. The inset in Fig. 5 shows the vessels with non-fluorinated and fluorinated suspensions (left and right vessels, respectively).

A common spectrum and carbon and fluorine related XPS spectra are shown in Fig. 7. A signal from fluorine F 1s was detected in the energy region of 687.7 eV in the spectra obtained HF-treated films. Such a position of the peak corresponds to  $sp^3$  hybridized chemically bound fluorine ions [18,23,24] and the bond has a covalent character [5,25]. For comparison, the position of the line of fluorine at 685.5 eV means that fluorine ions are bound with carbon by an ionic bond when carbon has  $sp^2$  hybridization. The energy position and shape of the peaks are indicative of partial fluorination of suspension particles (in the material, there remain carbon atoms not bound to fluorine) [26]. Carbon C 1s peak decomposition is given in Fig. 7 c-e. The appearance of peaks attributed to C-CF (285.6 eV), C-CF<sub>2</sub> (286.9 eV) and C-F (289.3) is observed [5,7,27]. An increase in the HF treatment time up to 60-70 days leads to the shift of C 1s peak position from 284.5 eV (C-C) to 285.6 eV (C-CF). The ratio between the areas under the peaks, due to carbon and fluorine for films treated in the HF-containing solution during 25 days (with allowance for different sensitivities of XPS to the two elements) corresponds to the formula C<sub>2</sub>F. Si- and O-related line intensity corresponds to native SiO<sub>2</sub> on the Si substrate with a thickness of 1-4 nm. Observation of the Si substrate with native SiO<sub>2</sub> on the surface was connected with the fact that tested area was larger than film size.

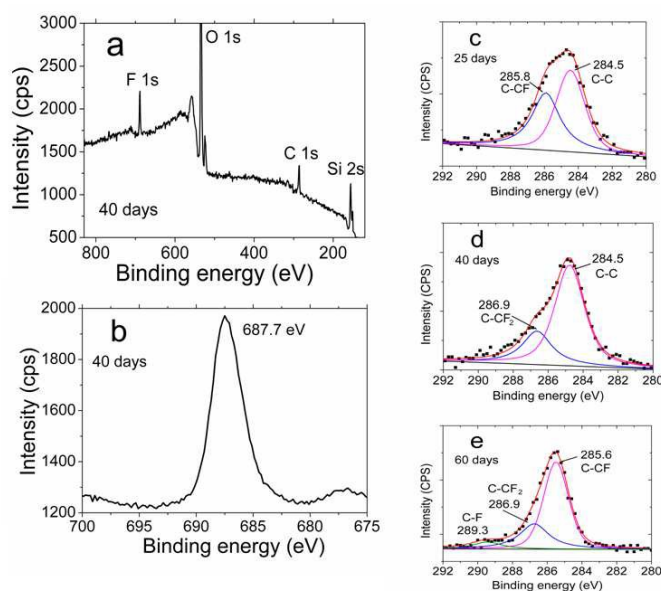


Fig. 7. (a) XPS spectra for the film created from suspension treated in the aqueous solution of HF during 40 days and (b) fluorine related XPS spectrum for the same film. F-1s spectra for all films had the same position. (c), (d), (e) Carbon related (C 1s) XPS spectra (points) for the films treated in the aqueous solution of HF during 25, 40, and 60 days, respectively. Fitting of XPS C 1s spectra (curves) with components mention in the figures.

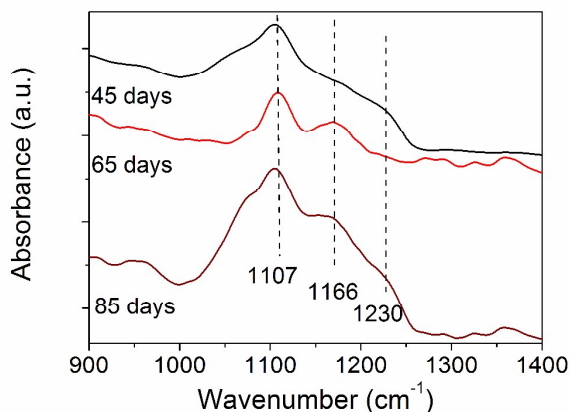


Fig. 8. FTIR spectra for some fluorinated films. Time of the treatment is given in the figure as a parameter.

The FTIR spectra obtained in the absorption mode for few fluorinated films are given in Fig.8. Strong IR bands with maxima 1107, 1166 and 1230  $\text{cm}^{-1}$  are clearly seen. When the fluorine atom is connected with  $\text{sp}^3$ -hybridization, the C–F bond is considered as covalent bonding, with the stretching vibration absorption corresponding to the peak at 1221  $\text{cm}^{-1}$  [27] or at 1260  $\text{cm}^{-1}$  [28]. For fluorographene exfoliated by N-methyl 2-pyrrolidone peaks 1212 and 1084  $\text{cm}^{-1}$  were observed corresponding to the stretching vibration of the C-F covalent bonds and the semi-ionic stretching vibration of C-F bonds, respectively [29]. The studies of FTIR spectra with an increasing fluorination time have revealed that an adsorption band at 1112  $\text{cm}^{-1}$  gradually changes into 1211  $\text{cm}^{-1}$  [30]. The modes observed in present study are suggested to correspond to those evaluated with a fluorination time C-F bond.

The stability of film electrical properties after thermal annealing in the temperature range 100–350°C allows us to state that oxidation does not occur during HF treatment.

A good chemical stability of obtained films is noteworthy. Additional treatments of structures with films on their surface in water, acetone and toluene were performed; such treatments caused no noticeable changes in the properties of fluorinated films.

### Dielectric properties of the films

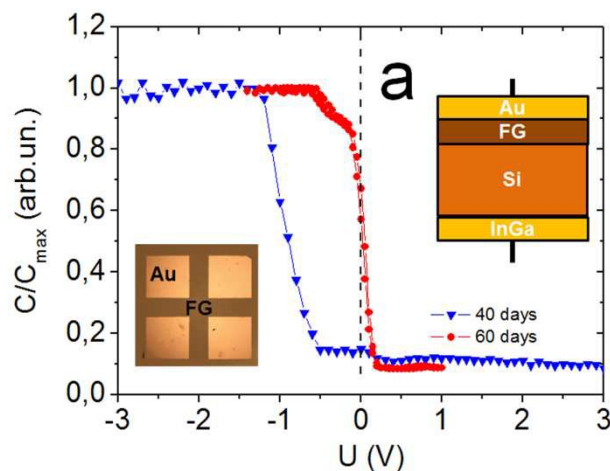
For measuring the capacitance-voltage characteristics, the obtained fluorographene films were provided with electrical contacts; such contacts were obtained by sputtering Au onto the film surface. Photograph of contacts and a sketch of obtained vertical MIS structures are presented in Fig. 9 a and in the insets to the figure.

The films prepared from the non-fluorinated suspension (0-day fluorination treatment) were conducting films. After HF treatment lasting during  $\sim 25$  days, the films proved to be dielectric films. The capacitance-voltage characteristic of an MIS structure measured at a frequency of 1 MHz with a graphene film fluorinated during 40 and 60 days are shown in Fig. 9. After 40-day fluorination treatment, the maximal

electric-field strength that could be withstood by the films, or the breakdown field strength, was  $\sim 1.2 \times 10^6$  V/cm. Increasing the duration of fluorination treatment resulted in a moderate increase of the breakdown voltage (within the range  $1.2 \times 10^6$  to  $3 \times 10^3$  V/cm). The values of the dielectric constant  $\epsilon$  of the films versus the duration of fluorination treatment are shown in insert of Fig. 8 b. For calculating those values, maximal capacitance (plateau) at capacitance-voltage characteristics  $C_m$  and film thickness  $d$  obtained by SEM and AFM, were used. Well-known equation for parallel-plate capacitor can be written as  $C_m = A\epsilon_0\epsilon/d$ , where  $\epsilon_0$  is the permittivity of vacuum,  $A$  is the surface area of contact. It is seen that the magnitude of  $\epsilon$  gradually approaches a value of 1.1. In [31], similar measurements performed on multilayer structures (up to 10 monolayers) of fluorographene have yielded for the dielectric constant a value  $\epsilon = 1.1$ . The graphite dielectric constant is known to be equal to 10 - 15. A number of models has been proposed and used for predicting the effects of second phases on the dielectric properties of the composites [32]. A changing in the dielectric constant of a composite, with respect to the filler concentration, can be explained by well established laws such as Bruggeman self-consistent effective medium approximation [33], Maxwell–Garnett equation [34] and other models [32,35]. We considered graphene inclusions as fillers and fluorographene as a matrix. From the value of the effective dielectric constant of partially fluorinated films, the relative degree of fluorination of suspension particles could be determined. For this purpose, in the present study we used relation [32,35]

$$\frac{\epsilon_{\text{exp}} - \epsilon_{\text{FG}}}{\epsilon_{\text{exp}} + 2\epsilon_{\text{FG}}} = v \frac{\epsilon_{\text{G}} - \epsilon_{\text{FG}}}{\epsilon_{\text{G}} + 2\epsilon_{\text{FG}}} \quad (1)$$

where  $\epsilon_{\text{exp}}$  is the experimentally evaluated dielectric constant of the partially fluorinated film,  $\epsilon_{\text{G}}$  and  $\epsilon_{\text{FG}}$  are graphene and fluorographene dielectric constants, and  $v$  is the graphene volume fraction. The degree of graphene fluorination was determined as  $(1 - v)$ . The obtained dependence for fluorination degree is shown in Fig. 8 b.



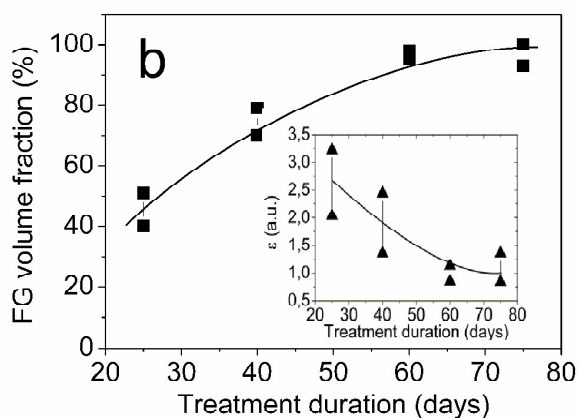


Fig. 9. (a) Capacitance-voltage characteristics of two Au-fluorographene-Si-InGa structures measured at 1-MHz frequency. The fluorographene films were obtained from suspension using fluorination procedures that lasted for 40 and 60 days. The inset at the right part of the figure shows a schematic representation of measured structure (Me are the metal contacts (Au on the fluorographene film and InGa alloy on the silicon substrate), Si is the silicon substrate, and FG is the fluorographene film). The rate of voltage sweep in measuring the capacitance-voltage characteristics was 0.03 V/s. The capacitance-voltage characteristic of the 60-day film was recorded by sweeping the voltage in two opposite directions; the data are indicative of no hysteresis. The inset at the left part of the figure shows the image of the film on the surface of silicon with Au contacts. The size of the square is 0.7 mm. (b) Film fluorination degree versus the duration of fluorination treatment in the solution of HF in water. The inset in Fig. 6 b shows the value of dielectric constant  $\epsilon$  versus the duration of the fluorination treatment.

The above relation is valid for gradually proceeding graphene fluorination in the fluorographene matrix with volume type of fillers. For the case of a high aspect ratio of graphene fillers (large graphene flakes), the dielectric constant of the composite is strongly changed already for a low nanosheets volume fraction (1-2%) [36]. In our case, the graphene fillers are suggested to have a small size and low aspect ratio of graphene or few-layer graphene flakes. This suggestion is based on the data of Fig. 8 and appearance of a photoluminescence from the film in the visible area which allows us to estimate the size of graphene fillers as  $\leq 10$  nm.

To evaluate the potential offered by the films under study as dielectric layers in thin-film device structures, we performed an analysis of the capacitance-voltage characteristics of MIS structures with such films with the aim to evaluate the fixed charge density in the film and the density of interface states at the film/Si substrate interface. The density of the fixed charge in the film  $Q_f$  was evaluated from the flat-band voltage as determined from the capacitance-voltage characteristics. The density of interface states at the interface with silicon  $D_{it}$  was determined from the difference between the charge  $Q_f$  and the charge  $Q_{mg}$  that was determined from the bias voltage at which the Fermi level took position at the middle of the bandgap of the semiconductor substrate. Recall that the fluorinated graphene film was applied onto a silicon surface free of native oxide. For films fluorinated during 25 days, the densities  $Q_f$  and

$D_{it}$  proved to be respectively  $(4-6) \times 10^{11} \text{ cm}^{-2}$  and  $(3-5) \times 10^{10} \text{ cm}^{-2}$ . On increasing the duration of fluorination treatment, the densities  $Q_f$  and  $D_{it}$  were found to decrease in value. In a film that was fluorinated during 65 days, the densities  $Q_f$  and  $D_{it}$  were found to be as low as  $\sim 5 \times 10^{10} \text{ cm}^{-2}$  and  $(1.5-3) \times 10^{10} \text{ cm}^{-2}$ , respectively; this finding proves that the quality of obtained dielectric films can be improved by increasing the treatment duration. On the whole, the obtained values proved to be much lower than the values of  $Q_f$  and  $D_{it}$  typical of many dielectric coatings used in nano- and microelectronics (for more detail, see Discussion).

## Discussion

The experimental data obtained in the present study using the various characterization techniques allow the following conclusions to be drawn: (1) Evidences for a fluorination reaction proceeding in examined graphene suspensions were obtained; such evidences involve the observed evolution of Raman spectra, XPS and FTIR data, change of suspension color, emergence of insulating properties in films, etc. In more details these evidences were discussed below. (2) Experimentally, a considerable reduction (reaching one-two orders of magnitude) of lateral and vertical sizes of suspension flakes treated in an aqueous solution of HF was revealed. Using the original fluorination process, thin (down to 20 nm), a really uniform insulating films with surface relief  $\sim 2$  nm were obtained from a graphene suspension. (3) The dielectric constant of the films (1.1 - 3.2), the breakdown field strength ( $\geq 10^6$  V/cm), the fixed charge in the film, and the density of states at the interface with silicon were evaluated. Fluorination and particle size reduction in the suspension are factors causing the observed changes in the properties of obtained films. On the basis of obtained direct and indirect data on the fluorination reaction proceeding between the HF-containing solution and graphene suspension particles, a model for the suspension fluorination process was proposed, and other processes proceeding during the treatment of suspension particles in an aqueous solution of HF were comprehended.

Let us consider in more details the evidences of graphene suspension fluorination under the treatment in aqueous solution of HF. Generally, an oxidation of graphene suspension under the HF treatment was assumed, and both variants (oxidation and fluorination) are considered. Nevertheless, only fluorination evidences were found. (1) The dielectric constant of the layers created from suspension after a long HF treatment was found to be equal to 1.1. It is exactly the same value of the dielectric constant that was found in [31] for fluorographene. Graphene oxide (GO) has a higher dielectric constant (4.3 [37]) and GO fillers are typically used for the creation of GO-polymer composites with a high dielectric constant [38]. (2) As was mentioned above, the temperature stability of the films created from the HF treated suspension was tested. It is well known that GO film resistivity is generally decreased starting with 100 - 200°C, whereas a decrease in FG film resistivity is observed at 400-450°C [18]. We have observed a decrease in



the film resistivity at temperature 400-450°C with activated energy 2,0 eV for HF-treated graphene or few-layer graphene samples (CVD, or mechanical exfoliation) [11]. For the films obtained from HF-treated suspension, isochronal annealing, again, demonstrates the stability of the properties up to 350°C. So, oxidation was not found from annealing experiments. (3) The colour of suspension after HF treatment changes from black to white (or more exactly to transparent), and not to brown, as typical of GO. (4) Raman measurements also prove fluorination rather than oxidation because all peaks are completely vanishing in the spectra. (5) XPS shows appearance of the F1s peak at the energy of 687.7 eV for the films from HF-treated suspensions. Such a position of the peak correspond to  $sp^3$  hybridized chemically bound fluorine ions [16,17,24]. Additional peaks near the C1s also correspond to C-CF, C-CF<sub>2</sub> and C-F bonds [5,7,27]. These peaks differed from the position of the peaks in grapheme oxide: C-O (286,2 eV), C=O (287.8 eV), C-OH [27,39,40]. It is worth mentioning here, that, in our case of treatment in the in aqueous solution of HF there are no peaks which correspond to CF<sub>2</sub> and C-F<sub>3</sub> typical of fluorination in the gas phase [5,7,18,27].

In the course of intercalation, the DMF dissolver penetrated in between flake layers, turning the flake s into layered structures. It is known that DMF does not interact chemically with graphene monolayers. An analysis of XPS spectra proves the absence of nitrogen in obtained films. The absence of the peak due to nitrogen in the XPS spectra of examined films confirms the fact that, in those films, in the presence of water DMF decomposes into formic acid (HCOOH) and gaseous formamide (HN(CH<sub>3</sub>)<sub>2</sub>) according to the reaction



The DMF decomposition reaction proceeding in the presence of water and HF is accompanied with the evolution of heat (342.8 kJ/mol, or 3.5 eV per each single reaction event) [41]. Expectedly, the evolved heat promotes the fluorination reaction according to the previously examined dependence of the rate of graphene and few-layer graphene fluorination on solution temperature [11]. Fluorination and the mismatch between graphene and fluorographene lattice constants (about 1%) lead to generation of mechanical stresses in the layers [18]. Relaxation of mechanical stresses results in deformation of fluorinated graphene layers and neighbor graphene regions. Following the deformation of the graphene, the graphene becomes more reactive, and its wettability with respect to the HF-containing solution increases [42, 43]. The wettability of fluorinated graphene with respect to water is higher in comparison with graphene. The change of flake surface wettability results in that the penetration of the HF-containing solution into flakes can become accelerated. As a result, fluorination of suspension particles leads to their additional exfoliation. The exfoliation and fractionation of suspension flakes is schematically shown in Fig. 3 c. The additional exfoliation makes the film and particle thicknesses decrease with treatment duration (see Figs. 1 – 4). Besides, as it follows

from Fig. 4 a, after a sufficiently long treatment the suspension contains, in addition to relatively coarse flakes sized 100 to 400 nm, fine particles sized 20 to 50 nm. In addition, the influence of fluorination on the properties of obtained films can be judged considering results of electrical measurements, which show that films obtained from suspensions treated for more than 25 days start displaying insulating properties brought about by the increased fluorination degree of the material.

It seems that, during the preparation of a suspension, DMF penetrated into 20 to 70 nm thick suspension particles only in between very few layers (typically, in between two-four monolayers). The intercalation was not complete, and it did not necessarily caused splitting of the material along intercalated layers. Treatment in hydrofluoric acid promoted the completion of DMF intercalation processes and caused addition exfoliation of suspension elements. Here, the expected minimal thickness of formed flakes is two-four monolayers; it is the very case that we observed in the experiment. It can be hypothesized that further fluorination will make possible splitting of particles into even thinner flakes. However, the latter reactions are expected to be processes proceeding much more slowly in comparison with the exfoliation of the material along DMF-intercalated layers.

XPS data (C1s peak decomposition for different samples) allow us to estimate the fluorination degree with use of area under the peaks. We have obtained formulas CF<sub>0,23</sub>, CF<sub>0,5</sub> and CF<sub>0,65</sub> for 25, 40 and 60 days of HF treatments, respectively. The fluorination degrees of the same films extracted from dielectric constant measurements (Fig.8b) are higher than that estimated from XPS data. The dielectric constant is the factor by which the electric field between the charges is decreased or increased related to vacuum. The presence of small few layer graphene fillers (with a relatively low aspect ratio) in the fluorinated matrix is found to have a weak effect on permittivity of the whole film. It is worth mentioning again that, in the case of a high aspect ratio of graphene fillers (large graphene flakes), the dielectric constant of the composite is strongly changed already for the 1-2% nanosheets volume fraction [36]. It allows us to assume that relatively large graphene flakes sized 100-400 nm are divided by fluorination on small graphene quantum dots.

The processes of chemical fragmentation of carbon materials with  $sp^2$ -hybridization are the well-known processes which, in particular, were used for obtaining nanoribbons out of carbon tubes [23,44]. The processes of chemical cutting of carbon nanotubes were a result of chemical oxidation of the nanotubes; this oxidation was first initiated at lattice defects and, then, it acted to «unzip» the tubes. Presently, similar processes are widely used for synthesizing graphene quantum dots sized 1 - 5 nm in diameter and exhibiting a strong photoluminescence [45-47]. It was assumed that, in aqueous solutions of various acids, the fractionation of particles in initial suspensions in finer particles was initiated in mechanically stressed regions of graphene sheets with high defect concentrations. Most actively, such processes proceed in autoclaves at elevated temperatures (~ 200°C) and pressures [3,18]. We believe that similar processes proceeded in the suspensions examined in the present

study. As it follows from the high amplitude of the D peak in Raman spectra, the graphite and few-layer graphene particles contained a substantial amount of structural defects (Figs. 6 a and 6 b). Those defects could be introduced into the material at any suspension preparation stage, be that the mechanical crushing, the DMF dissolver intercalation, or the ultrasonic treatment. During fluorination, the defects are expected to be initiation sites for the reaction of fluorination of suspension flakes and, subsequently, flake rupture points. It seems that finer suspension particles sized 20 to 50 nm serve an analogue of quantum dots in the well-known graphene fractionation processes. In the case treated in the present study, large sizes of such flakes were the consequence of the fact that the reaction was held at normal conditions (comparatively low temperature and/or pressure). Simultaneously, the suspension also contained coarse round flakes, close in their sizes (100-400 nm), who were the basic suspension elements. Very probably, a more intricate shape of particles would lead to higher mechanical stresses generated at bent surface regions, which can be considered defects present at the boundary and promoting the cutting of fragments from the surface.

Unique properties of the dielectric films obtained from the fluorinated suspension are noteworthy. The value of the fixed charge,  $\sim 5 \times 10^{10} \text{ cm}^{-2}$ , and the density of interface states,  $\sim 2 \times 10^{10} \text{ cm}^{-2}$ , can be regarded as excellent values for a dielectric film. Such values can only be reached in  $\text{SiO}_2$  layers, featuring a well-established fabrication technology. All other known dielectric films, including  $\text{Si}_3\text{N}_4$ ,  $\text{Al}_2\text{O}_3$ ,  $\text{HfO}_2$  etc., yield the charge and interface-state densities of  $10^{11} - 10^{12} \text{ cm}^{-2}$ . So, we have obtained the minimum possible charge density in a film. Besides, the films withstand the high electric field strengths of  $(1-3) \times 10^6 \text{ V/cm}$ . A breakdown field strength  $10^7 \text{ V/cm}$  was obtained for fluorographene films produced from graphene and few-layered graphene in fluorine-containing plasma [31]. The obtained values of the dielectric constant of fluorinated films ( $\epsilon = 3 - 2$  for the moderate fluorination duration of 25 - 40 days and  $\epsilon = 1.1$  for the sufficiently long fluorination duration of 60-70 days and, hence, different fluorination degrees) varies from values close to the value of  $\epsilon$  for amorphous fluorinated graphite ( $\sim 2.1$ ) as determined from similar measurements [48] to the value 1.1 obtained for few-layer fluorographene structures [31].

On the whole, the obtained dielectric films exhibit good structural and electrical properties. Owing to the simple preparation procedure of such films and easiness of their application onto substrates, and also owing to the possibility of obtaining very thin layers, fluorinated graphene films offer promise in application as dielectric layers in thin-film device structures.

## Conclusions

The processes proceeding during the interaction of DMF-based graphene suspension with a solution of hydrofluoric acid in water were studied. It was found that, as a result of the interaction, the suspension particles undergo an additional splitting (up to 1-5 monolayers) and size reduction (100-300

nm). Evidences proving the fluorination of suspension flakes during the treatment of the suspension in an aqueous solution of HF in water are based on the evolution of Raman spectra, XPS and FTIR data, change of suspension color, emergence of insulating film properties. A schematic pattern for the joint action of DMF and the HF-containing solution for suspension, flakes resulting in additional exfoliation of graphene sheets and formation of thinner and finer fluorinated graphene particles was proposed.

From the fluorinated suspension, thin (100 - 20 nm), a really uniform insulating films were obtained. The films exhibit a surface relief of  $\sim 2 \text{ nm}$  high, and they can be applied onto arbitrarily large areas. The film dielectric constant of the films was determined to be equal to 3.2 down to 1.1 depending on the fluorination degree of the material. It was shown that films prepared from a fluorinated suspension exhibit high breakdown fields ( $> 1 \times 10^6 \text{ V/cm}$ ), and they contain low charge densities in the film and at the interface with silicon in metal-dielectric-semiconductor structures, the fixed charge density in the film and the density of interface states being  $\sim (1-5) \times 10^{10} \text{ cm}^{-2}$ . Such excellent characteristics of the dielectric film (high breakdown electrical field and low densities of charges) make them promising layers for the use as insulating elements in thin-film device structures. Moreover, the films from the fluorinated suspension are cheap, practically feasible and easy to produce.

## Acknowledgements

This work was supported in part by the Russian Foundation for Basic Research (Grant No. 14-32-50270), by Siberian Branch of Russian Academy of Sciences (Project 75) and by the Ministry of Science and Education of the Russian Federation.

## Notes and references

- a Rzhanov Institute of Semiconductor Physics, Russian Academy of Science, Siberian Division, 630090, Novosibirsk, Acad. Lavrent'ev Avenue, 13.  
 b Novosibirsk State University, 630090, Novosibirsk, Pirogov Street, 2.  
 c Ammosov North-Eastern Federal University, 677000, Yakutsk, Belinskii Street, 58.
1. K. S. Novoselov, V. I. Fal'ko, L. Colombo, P. R. Gellert, M. G. Schwab, K. Kim. A roadmap for graphene, *Nature*, 2012, **490**(7419), 18-200.
  2. E. Bekyarova, S. Sarkar, S. Niyogi, M. E. Itkis, R. C. Haddon. Advances in the chemical modification of epitaxial graphene, *Journal of Physics D: Applied Physics*, 2012, **45**, 154009.
  3. M. Bacon, S. J. Bradley, T. Nann. Graphene quantum dots, *Particle & Particle Systems Characterization*, 2014, **31**(4), 415-28.
  4. P. Sessi, J. R. Guest, M. Bode, N. P. Guisinger. Patterning Graphene at the Nanometer Scale via Hydrogen Desorption, *Nano Letters*, 2009, **9**(12), 4343-7.
  5. J. T. Robinson, J. S. Burgess, C. E. Junkermeier, S. C. Badescu, T. L. Reinecke, F. K. Perkins, M. K. Zalalutdniov, J. W. Baldwin, J. C. Culbertson, P. E. Sheehan, E. S. Snow. Properties of Fluorinated Graphene Films, *Nano Letters*, 2010, **10**(8), 3001-5.

6. Md. Z. Hossain, J. E. Johns, K. H. Bevan, H. J. Karmel, Y. T. Liang, S. Yoshimoto, K. Mukai, T. Koitaya, J. Yoshinobu, M. Kawai, A. M. Lear, L. L. Kesmodel, S. L. Tait, M. C. Hersam. Chemically homogeneous and thermally reversible oxidation of epitaxial graphene, *Nature Chemistry*, 2012, **4**(4), 305-9.
7. Z. Wang, J. Wang, Z. Li, P. Gong, X. Liu, L. Zhang, J. Ren, H. Wang, S. Yang. Synthesis of fluorinated graphene with tunable degree of fluorination, *Carbon*, 2012, **50**(15), 5403-10.
8. M. Bruna, B. Massessi, C. Cassiogo, A. Battiato, E. Vittone, G. Speranzad, S. Borini. Synthesis and properties of monolayer graphene oxyfluoride, *Journal of Materials Chemistry*, 2011, **21**(46), 18730-37.
9. O. Ö. Ekiz, M. Ürel, H. Güner, A. K. Mizrak, A. Dâna. Reversible electrical reduction and oxidation of graphene oxide, *ACS Nano*, 2011, **5**(4), 2475-82.
10. Y. Yang, G. Lu, Y. Li, Z. Liu, X. Huang, One-step preparation of fluorographene: a highly efficient, low-cost, and large-scale approach of exfoliating fluorographite. *ACS Appl Mater Interfaces*, 2013, **5**(24), 13478-83
11. N. A. Nebogatikova, I. V. Antonova, V. Ya. Prinz, V. A. Volodin, D. A. Zatsepin, E. Z. Kurmaev, I. S. Zhidkov, S. O. Cholakh. Functionalization of graphene and few-layer graphene films in an hydrofluoric acid aqueous solution, *Nanotechnologies in Russia*, 2014, **9**(1-2), 51-9.
12. N. A. Nebogatikova, I. V. Antonova, V. Ya. Prinz. Functionalization of graphene and few-layer graphene with aqueous solution of hydrofluoric acid, *Physica E: Low-dimensional Systems and Nanostructures*, 2013, **52**, 106-11.
13. L. Britnell, R. V. Gorbachev, A. K. Geim, L. A. Ponomarenko, A. Mishchenko, M. T. Greenaway, T. M. Fromhold, K. S. Novoselov, L. Eaves. Resonant tunnelling and negative differential conductance in graphene transistors, *Nature Communications*, 2013, **4**, 1794.
14. A. N. Sidorov, M. M. Yazdanpanah, R. Jalilian, P. J. Ouseph, R. W. Cohn, G. U. Sumanasekera. Electrostatic deposition of graphene, *Nanotechnology*, 2007, **18**(13), 135301-5.
15. F. Bonaccorso, A. Lombardo, T. Hasan, Z. Sun, L. Colombo, A. C. Ferrari. Production and processing of graphene and 2d crystals, *Materials Today*, 2012, **15**(12), 564-89.
16. S. Y. Oh, S. H. Kim, Y. S. Chi, T. J. Kang. Fabrication of oxide-free graphene suspension and transparent thin films using amide solvent and thermal treatment, *Applied Surface Science*, 2012, **258**(22), 8837-44.
17. M. Zhou, T. Tian, X. Li, X. Sun, J. Zhang, P. Cui, J. Tang, L. Ch. Qin. Production of graphene by liquid-phase exfoliation of intercalated graphite, *International journal of electrochemical science*, 2014, **9**, 810-20.
18. R. R. Nair, W. Ren, R. Jalil, I. Riaz, V. G. Kravets, L. Britnell, P. Blake, F. Schedin, A. S. Mayorov, S. Yuan, M. I. Katsnelson, H. M. Cheng, W. Strupinski, L. G. Bulusheva, A. V. Okotrub, I. V. Grigorieva, A. N. Grigorenko, K. S. Novoselov, A. K. Geim. Fluorographene: a two-dimensional counterpart of Teflon, *Small*, 2010, **6**(24), 2877-84.
19. N. A. Nebogatikova, I. V. Antonova, V. Ya. Prinz, V. B. Timofeev, S. A. Smagulova, Graphene quantum dots in fluorographene matrix formed by means of chemical functionalization, *Carbon*, 2014, **77**, 1095-103.
20. S. F. Tayyari, H. Reissi, F. Milani-Nejad, I. S. Butler. Vibrational assignment of  $\alpha$ -cyanoacetylacetone, *Vibrational Spectroscopy*, 2001, **26**(2), 187-99.
21. S. E. Fisher, J. M. Chalmers, A. Marcelli, H. J. Byrne, F. Lyng, P. Lasch, L. M. Miller, P. Dumas, P. Gardner, D. Moss. Biomedical Applications of Synchrotron Infrared Microspectroscopy (RSC Analytical Spectroscopy), *Royal Society of Chemistry*, 2010.
22. P. B. Nagabalasubramanian, S. Periandy, S. Mohan. A scaled quantum mechanical approach of vibrational analysis of o-tolunitrile based on FTIR and FT Raman spectra, ab initio, Hartree Fock and DFT methods, *Spectrochimica Acta Part A: Molecular and Biomolecular Spectroscopy*, 2009, **74**(5), 1280-7.
23. V. N. Khabashesku. Covalent functionalization of carbon nanotubes: synthesis, properties and applications of fluorinated derivatives, *Russian Chemical Reviews*, 2011, **80**, 705-28.
24. S. D. Sherpa, G. Levitin, D. W. Hess. Effect of the polarity of carbon-fluorine bonds on the work function of plasma-fluorinated epitaxial graphene, *Applied Physics Letters*, 2012, **101**, 111602.
25. N. O. Plank, L. Jiang, R. Cheung. Fluorination of carbon nanotubes in CF<sub>4</sub> plasma, *Applied Physics Letters*, 2003, **83**, 2426-8.
26. G. Tsoukleri, J. Parthenios, K. Papagelis, R. Jalil, A. C. Ferrari, A. K. Geim, K. S. Novoselov, C. Galiotis. Subjecting a graphene monolayer to tension and compression, *Small*, 2009, **5**, 2397-2402.
27. X. Wang, Y. Dai, J. Gao, J. Huang, B. Li, C. Fan, J. Yang, X. Liu, High-Yield Production of Highly Fluorinated Graphene by Direct Heating Fluorination of Graphene-oxide, *ACS Applied Materials & Interfaces*, 2013, **5**, 8294-9.
28. F. Karlick, K. Kumara R. Datta, M. Otyepka, R. Zboril, Halogenated graphenes: rapidly grown family of graphene derivatives. *ACS Nano*, 2013, **7**, 64343-64.
29. P. W. Gong, Z. F. Wang, J. Q. Wang, H. G. Wang, Z. P. Li, Z. J. Fan, Y. Xu, X. X. Han, S. R. Yang. One-pot sono-chemical preparation of fluorographene and selective Tuning of its fluorine coverage. *Journal of Materials Chemistry*, 2012, **22**, 16990-6.
30. Y. Wang, W. C. Lee, K. K. Manga, P. K. Ang, J. Lu, Y. P. Liu, C. T. Lim, K. P. Loh Fluorinated graphene for promoting neuro-induction of stem cells. *Advanced Materials*, 2012, **24**, 4285-90.
31. K. I. Ho, C. H. Huang, J. H. Liao, W. Zhang, L. J. Li, C. S. Lai, C. Y. Su. Fluorinated Graphene as High Performance Dielectric Materials and the Applications for Graphene Nanoelectronics, *Scientific Reports*, 2014, **4**, 5893.
32. Z.-M. Dang, J.-K. Yuan, J.-W. Zha, T. Zhou, S.-T. Li, G.-H. Hu. Fundamentals, processes and applications of high-permittivity polymer-matrix composites. *Progress in Materials Science*, 2012, **57**, 660-723
33. D. A. G. Bruggeman. The calculation of various physical constants of heterogeneous substances. I. The dielectric constants and conductivities of mixtures composed of isotropic substances. *Ann Phys*, 185, **24**, 636-42.
34. C. W. Nan. Comment on 'Effective dielectric function of a random medium'. *Physical Review B*, 2001, **63**, 176201.
35. Z.-M. Dang, J.-K. Yuan, S.-H. Yao, R.-J. Liao. Flexible nanodielectric materials with high permittivity for power energy storage. *Advanced Materials*, 2013, **25**(44), 6334-65.
36. D. Wang, T. Zhou, J.-W. Zha, Z.-M. Dang. Functionalized graphene - BaTiO<sub>3</sub> / ferroelectric polymer nanodielectric composites with high permittivity, low dielectric loss, and low percolation threshold. *Journal of Materials Chemistry A* 2013, **1**, 6162 - 8.
37. B. Standley, A. Mendez, E. Schmidgall, M. Bockrath, Graphene-Graphite Oxide Field-Effect Transistors, *Nano Lett.*, 2012, **12**, 1165-9.
38. J.-Y. Kim, J. Lee, W.H. Lee, I.N. Kholmanov, J.W. Suk, T.Y. Kim, Y. Hao, H. Chou, D. Akinwande, R.S. Ruoff. Flexible and Transparent Dielectric Film with a High Dielectric Constant Using Chemical Vapor Deposition-Grown Graphene Interlayer *ACS Nano*, 2014, **8**, 269-74.
39. S. Mao, K. Yu, S. Cui, Z. Bo, G. Lu, J. Chen A new reducing agent to prepare single-layer, high-quality reduced graphene oxide for device applications. *Nanoscale*, 2011, **3**, 2849-53.

40. V.H. Pham, H.D. Pham, T.T. Dang, S.H. Hur, E.J. Kim, B.S. Kong, S. Kima, J.S. Chung. Chemical reduction of an aqueous suspension of graphene oxide by nascent hydrogen. *J. Mater. Chem.*, 2012, **22**, 10530-6.
41. P. W. Atkins, P. J. De. Atkins' Physical chemistry, *Oxford: Oxford University Press*, 2006.
42. W. Xiong, J. Z. Liu, Zh. L. Zhang, Q. S. Zhen. Control of surface wettability via strain engineering, *Acta Mechanica*, 2013, **29(4)**, 543–9.
43. D. W. Boukhvalov, M. I. Katsnelson. Chemical functionalization of graphene, *Journal of Physics: Condensed Matter*, 2009, **21(34)**, 344205
44. Z. Gu, H. Peng, R. H. Hauge, R. E. Smalley, J. L. Margrave. Cutting single-wall carbon nanotubes through fluorination. *Nano Letters*. 2002, **2(9)**, 1009-13.
45. Z. Chen, T. Huang, B. C. Jin, J. Hu, H. Lu, S. Nutt. High yield synthesis of single-layer graphene microsheets with dimensional control, *Carbon*. 2014, **68**, 164-74.
46. H. Tetsuka, R. Asahi, A. Nagoya, K. Okamoto, I. Tajima, R. Ohta, A. Okamoto. Optically tunable amino-functionalized graphene quantum dots, *Advanced Materials*, 2012, **24(39)**, 5333-8.
47. M. Xu, Z. Li, X. Zhu, N. Hu, H. Wei, Z. Yang, Y. Zhang. Hydrothermal / solvothermal synthesis of graphene quantum dots and their biological applications, *Nano Biomedicine & Engineering*, 2013, **5(2)**, 65-71.
48. Y. Ma, H. Yang, J. Guo, C. Sathe, A. Agui, J. Nordgren. Structural and electronic properties of low dielectric constant fluorinated amorphous carbon films, *Applied Physics Letters*, 1998, **72**, 3353-5.